Title

Analysis of the contribution of MTP and the predicted Flp pilus genes to Mycobacterium tuberculosis pathogenesis

Journal

Microbiology, 162(10)

ISSN

1350-0872

Authors

Mann, Katherine M
Pride, Aaron C
Flentie, Kelly
et al.

Publication Date

2016-10-01

DOI

10.1099/mic.0.000368

Peer reviewed

Microbiology (2016), **162**, 1784–1796 **DOI** 10.1099/mic.0.000368

Analysis of the contribution of MTP and the predicted Flp pilus genes to *Mycobacterium tuberculosis* pathogenesis

Katherine M. Mann, Aaron C. Pride, Kelly Flentie, Jacqueline M. Kimmey, Leslie A. Weiss and Christina L. Stallings

Department of Molecular Microbiology, Washington University School of Medicine, St. Louis, MO 63110, USA

Correspondence
Christina L. Stallings
stallings@wusm.wustl.edu

Received 19 August 2016
Accepted 30 August 2016

Mycobacterium tuberculosis (Mtb) is one of the world's most successful pathogens. Millions of new cases of tuberculosis occur each year, emphasizing the need for better methods of treatment. The design of novel therapeutics is dependent on our understanding of factors that are essential for pathogenesis. Many bacterial pathogens use pili and other adhesins to mediate pathogenesis. The recently identified *Mycobacterium tuberculosis* pilus (MTP) and the hypothetical, widely conserved Flp pilus have been speculated to be important for Mtb virulence based on *in vitro* studies and homology to other pili, respectively. However, the roles for these pili during infection have yet to be tested. We addressed this gap in knowledge and found that neither MTP nor the hypothetical Flp pilus is required for Mtb survival in mouse models of infection, although MTP can contribute to biofilm formation and subsequent isoniazid tolerance. However, differences in *mtp* expression did affect lesion architecture in infected lungs. Deletion of *mtp* did not correlate with loss of cell-associated extracellular structures as visualized by transmission electron microscopy in Mtb Erdman and HN878 strains, suggesting that the phenotypes of the *mtp* mutants were not due to defects in production of extracellular structures. These findings highlight the importance of testing the virulence of adhesion mutants in animal models to assess the contribution of the adhesin to infection. This study also underscores the need for further investigation into additional strategies that Mtb may use to adhere to its host so that we may understand how this pathogen invades, colonizes and disseminates.

INTRODUCTION

Mycobacterium tuberculosis (Mtb) is one of the leading infectious causes of death worldwide, resulting in 9.6 million new tuberculosis (TB) cases and 1.5 million deaths in 2014 (WHO, 2015). High rates of TB disease and multidrug resistance emphasize the need for better therapeutics to combat this deadly pathogen. The design of new drugs will be informed by our understanding of the factors required for Mtb pathogenesis.

Abbreviations: CR, Congo red; d.p.i., days post-infection; H&E, haematoxylin and eosin; HBHA, heparin-binding haemagglutinin adhesion protein; INH, isoniazid; Mtb, *Mycobacterium tuberculosis*; MTP, *Mycobacterium tuberculosis* pilus; NEC, necrosis-associated extracellular cluster; qRT-PCR, quantitative real-time PCR; TB, tuberculosis; TEM, transmission electron microscopy; c.f.u., colony forming units.

Three supplementary figures are available with the online Supplementary Material.

Adhesins, which are cell surface molecules used for adherence, are essential for the virulence of many bacterial pathogens (Barocchi *et al.*, 2006; Connell *et al.*, 1996; Khelef *et al.*, 1994; Mulvey *et al.*, 2001; Nielsen *et al.*, 2012; Schreiner *et al.*, 2003; Taylor *et al.*, 1987; Terao *et al.*, 2012). Bacterial adhesins play roles in attachment, entry, invasion (Mandlik *et al.*, 2008; Pizarro-Cerdá *et al.*, 2006), tropism (Wright & Hultgren, 2006) and colonization of host cells (Mandlik *et al.*, 2008). In addition, adhesins are often important for biofilm formation (Flores-Mireles *et al.*, 2015; Foster *et al.*, 2014; Mandlik *et al.*, 2008; Telford *et al.*, 2006), signal transduction (Moorthy *et al.*, 2016), immune activation (Blanco *et al.*, 2012; Lee *et al.*, 2005; Mandlik *et al.*, 2008) and immune evasion (Flores-Mireles *et al.*, 2015; Foster *et al.*, 2014; Nobbs *et al.*, 2009).

While several Mtb proteins have been classified as adhesins [recently reviewed in Govender *et al.* (2014)], their functional roles are often largely unclear. In particular, two types of pili have been recently reported in Mtb. Pili were initially investigated in Gram-negative bacteria, and it was long

thought that Mtb did not express a pilus. Several years ago, it was reported that the *Mycobacterium tuberculosis* pilus (MTP) (encoded by *Rv3312a*) is present in multiple strains of Mtb (Alteri *et al.*, 2007). MTP binds laminin, can be recognized by immune sera from active TB patients (Alteri *et al.*, 2007) and resembles curli, which are extracellular proteinaceous fibres produced by many Enterobacteriaceae that share biochemical properties with amyloid (Barnhart & Chapman, 2006; Blanco *et al.*, 2012). The potential importance of MTP as a Mtb virulence factor and biomarker (Naidoo *et al.*, 2014) has spurred research from multiple groups and has led to a number of reviews on mycobacterial adhesins (Govender *et al.*, 2014; Hosseini *et al.*, 2014; Ramsugit & Pillay, 2015). Recent studies using a clinical isolate of Mtb, V9124, have shown that an *mtp* deletion mutant is defective in *in vitro* pellicle biofilm formation (Ramsugit *et al.*, 2013) and in adherence to and invasion of A549 epithelial cells (Ramsugit *et al.*, 2016), but it has no defect in adhering to and invading THP-1 macrophages (Ramsugit & Pillay, 2014). These same studies also show that a V9124 *mtp* complemented overexpression strain forms normal biofilms (Ramsugit *et al.*, 2013), adheres to and invades A549 epithelial cells similarly to WT bacteria (Ramsugit *et al.*, 2016) and has enhanced invasion and adherence to THP-1 macrophages (Ramsugit & Pillay, 2014). However, the biological relevance of MTP during Mtb pathogenesis has not been directly tested, and it should be noted that the characterization of MTP as an extracellular structure is limited to two publications (Alteri *et al.*, 2007; Ramsugit *et al.*, 2013).

In addition to the *mtp* gene, the genome of Mtb also contains the *tad* (tight adherence) operon, which encodes the components of a type IV pilin assembly system known as the Flp pilus, named for its major structural pilin protein Flp (Kachlany *et al.*, 2000). The *tad* locus is widely distributed in many bacterial and all archaeal genomes and was originally identified in the Gram-negative oral pathogen *Aggregatibacter actinomycetemcomitans*, where it is essential for tight adherence, autoaggregation, rough colony morphology and virulence (Kachlany *et al.*, 2001; Planet *et al.*, 2003; Schreiner *et al.*, 2003). Although the *tad* operon consists of 14 genes in *A. actinomycetemcomitans*, Mtb has only maintained five genes of the *tad* operon: *tadZ*, encoding an inner membrane-associated cytoplasmic ATPase-like protein potentially involved in pilin localization; *tadA*, encoding an inner membrane ATPase that drives pilin assembly; *tadB* and *tadC*, encoding proteins that may serve as a secretion apparatus and the major *flp* pilin gene (Tomich *et al.*, 2007). Additionally, two predicted pseudopilin genes adjacent to the *tadZABC-flp* locus in Mtb encode proteins with partial homology to TadE and TadF in *A. actinomycetemcomitans*. However, the proteins encoded by these genes are missing the conserved N-terminal G/XXXXEF motif found in other pseudopilins (Kachlany *et al.*, 2000) and, therefore, have been disregarded as true members of the *tad* system in Mtb. It has been speculated that this predicted Flp pilus could contribute to Mtb pathogenesis (Alteri, 2005; Ramsugit & Pillay, 2015), but this has not been investigated.

Despite the recent attention that MTP and the predicted Flp pilus have gained, roles for Mtb pili in pathogenesis thus far have only been speculated. In this study, we address this gap in knowledge by testing the virulence of Mtb Erdman strain *mtp* and *flp* mutants in mouse models of infection. Importantly, we also examine whether phenotypes of these mutants correlate with loss of cell-associated extracellular structures resembling pili.

METHODS

Bacterial strains and growth conditions. Mtb strains Erdman and HN878 and their derivatives were cultured at 37 °C in Middlebrook 7H9 (broth) or Middlebrook 7H10 (agar) supplemented with 10 % oleic acid/albumin/dextrose/catalase, 0.5 % glycerol and 0.05 % Tween 80 (7H9 only) or in Sauton's liquid medium. When needed, Congo red (CR; Sigma) was added to 7H10 plates at a concentration of 100 μg ml^{-1} (Parrish *et al.*, 2004). Bacterial biofilms were inoculated with stationary phase planktonic cultures into Sauton's medium at a 1 : 100 dilution. Culture vessels were closed tightly to restrict oxygen for 3 weeks and then vented as previously described (Ojha *et al.*, 2008). Rugose colony biofilms were formed by pipetting 5 μl of stationary phase planktonic Mtb on agar plates. In mycobacterial cultures, 20 μg ml^{-1} kanamycin, 50 μg ml^{-1} hygromycin and isoniazid (INH) at indicated concentrations were supplemented as needed.

Construction of mutant strains. For the creation of the Mtb Δ*mtp* strains in the Erdman and HN878 background, a specialized transducing phage containing homology to the Mtb H37Rv reference genome nucleotides 3701044 to 3701747 and 3700108 to 3700707 was used to replace the endogenous *mtp* gene with a hygromycin resistance cassette. Mutants were confirmed by Southern blotting. The Δ*mtp*+*mtp* complemented strain that constitutively expresses *mtp* was created by integrating pMSG430 *mtp* into the *attB* site of the Δ*mtp* strain. The Δ*mtp* +*empty* vector control strain was created by integrating pMSG430 into the *attB* site of the Δ*mtp* strain (see Fig. S1, available in the online Supplementary Material).

Creation of strains deficient in various components of the *tad* locus/Flp pilus was carried out in the same way. Specialized transducing phage containing homology to Mtb nucleotides 4097979 to 4098656 and 4095482 to 4096119 was created for the deletion of *tadA* and *tadB*, while phage containing homology to Mtb nucleotides 4096132 to 4096762 and 4094636 to 4095323 was used for the deletion of *tadC* and *flp*.

Crystal violet staining. Mtb biofilm biomass was quantified by adapting previously published protocols (O'Toole & Kolter, 1998). Cultures were grown under pellicle biofilm-forming conditions in 96-well plates, media were aspirated and plates were gently washed with water three times. Plates were stained with 0.5 % crystal violet for 15 min, washed three times in water and air dried. To quantify staining, we used 45 % acetic acid to de-stain each well, diluted at 1 : 10 in formalin and read at $OD\lambda_{570}$.

Stress and tolerance assays. Mtb was grown under biofilm-forming conditions in 24-well plates in Sauton's medium. After 3 weeks, seals on the vessels were opened and concentrated solutions of INH or water control were pipetted underneath the surface of the culture. After 2 weeks of exposure to the indicated stress, bacteria were harvested from each well, centrifuged to pellet and resuspended in 1 % Tween 80 in PBS. Glass beads were added to each tube and tubes were shaken overnight at room temperature to disassociate bacteria. Serial dilutions were

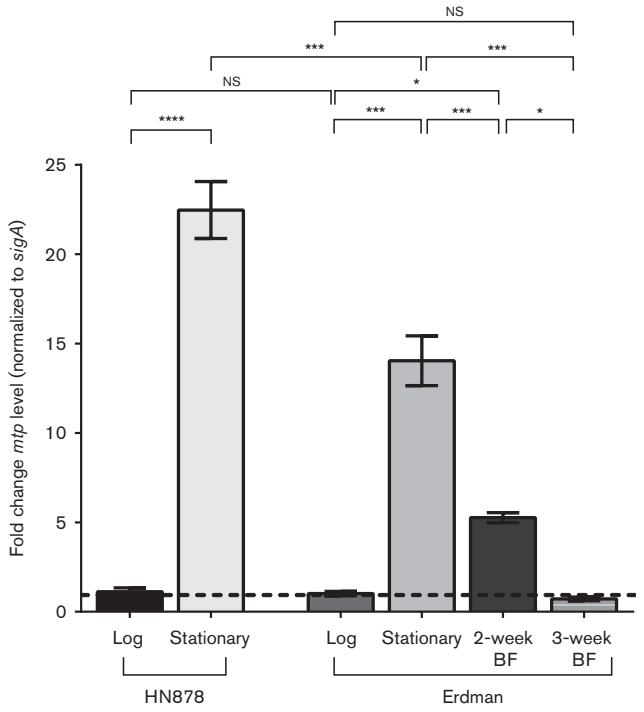

Fig. 1. *mtp* transcript levels. *mtp* transcript levels in Mtb HN878 WT and Erdman WT logarithmic (log) and stationary planktonic cultures, as well as 2- and 3-week (wk) Erdman biofilm (BF) cultures were measured by qRT-PCR, normalized to *sigA* transcript levels and expressed as a fold change from Erdman log phase cultures. Each bar represents triplicate biological replicates except 3-week BF, which represents duplicate biological replicates. Graphical data in this and subsequent figures are represented as mean±SEM. Statistical differences were determined by one-way ANOVA and Tukey's multiple comparison test. *$P<0.05$, **$P<0.01$, ***$P<0.001$ and ****$P<0.0001$; NS, not significant.

plated to enumerate c.f.u. For planktonic stress tolerance assays, bacteria were cultured into 7H9 medium containing 0.05 % Tween 80 and grown for 14 days in 96-well plates at 37 °C. After 14 days, bacteria were harvested and serial dilutions were plated to enumerate c.f.u. and determine survival.

Quantitative real-time PCR. RNA was isolated from mycobacteria using Trizol (Invitrogen) and chloroform followed, by either isopropanol and high salt precipitation or extraction with the Direct-Zol RNA Miniprep (Zymo Research). DNA was removed using the TURBO DNA-free kit (ThermoFisher Scientific), cDNA was prepared using Superscript III (Invitrogen) and quantitative real-time PCR (qRT-PCR) was performed using iTaq Universal SYBR Green Supermix (Bio-Rad). Primers used to amplify *mtp* were 5′-TGCCCGACTACTACTGGTGCC-3′ and 5′-CACGGGACCTTCGAGGATGGG-3′. Levels of *mtp* transcript were normalized to *sigA* transcript levels as previously described (Stallings *et al.*, 2009).

Negative staining and analysis by electron microscopy. Biomass from Mtb rugose colony biofilms or pellicle biofilms was collected into 4 % paraformaldehyde (Electron Microscopy Sciences) and vortexed. Samples were allowed to absorb onto glow-discharged formvar/carbon-coated copper grids. Grids were washed in distilled water and stained with 1 % aqueous uranyl acetate (Ted Pella) for 1 min. Excess liquid was gently wicked off and grids were allowed to air dry. Samples were viewed on a JEOL 1200EX transmission electron microscope (TEM; JEOL) equipped with an AMT 8 megapixel digital camera (Advanced Microscopy Techniques).

Mouse infections. Before infection, exponentially replicating Mtb strains were washed in PBS+0.05 % Tween 80 and were sonicated to disperse clumps. Female C3HeB/FeJ or C57Bl/6 mice 8–9 weeks old (Jackson Laboratory) were exposed to 8×10^7 c.f.u. of the appropriate strain in a Middlebrook Inhalation Exposure System (Glas-Col), which delivers ~100 bacteria per animal. Bacterial burden was determined by plating serial dilutions of lung and spleen homogenates onto 7H10 agar plates. Plates were incubated at 37 °C in 5 % CO_2 for 3 weeks prior to counting colonies. For histology, mouse lungs were fixed and stored in 10 % buffered formalin until processing. Lungs were then dehydrated using ethanol and processed by the Department of Internal Medicine–Pulmonary Disease Pulmonary Morphology Core, where they were paraffin embedded and sectioned, and consecutive sections were stained with either haematoxylin and eosin (H&E) stain or acid-fast stain. Slides were visualized using an Olympus BX51 light microscope (Olympus) equipped with a MicroPublisher 5.0 digital camera (Q Imaging).

All mice in this manuscript survived unless humanely sacrificed to measure bacterial burden and histological signs of disease.

All procedures involving animals were conducted following the National Institutes of Health guidelines for housing and care of laboratory animals and performed in accordance with institutional regulations after protocol review and approval by the Institutional Animal Care and Use Committee of Washington University in St. Louis School of Medicine (protocol no. 20130156, Analysis of Mycobacterial Pathogenesis). Washington University is registered as a research facility with the United States Department of Agriculture and is fully accredited by the American Association of Accreditation of Laboratory Animal Care. The Animal Welfare Assurance is on file with the National Institutes of Health's (NIH) Office for Protection from Research Risks. All animals used in these experiments were subjected to no or minimal discomfort. All mice were euthanized by CO_2 asphyxiation, which is approved by the American Veterinary Association Panel on Euthanasia.

RESULTS

mtp expression changes based on growth phase

To investigate when MTP may be functioning in Mtb, we first monitored *mtp* expression at different phases of bacterial growth in two different strains of Mtb, the laboratory strain Erdman of the Euro-American lineage and the hypervirulent HN878 strain of the W-Beijing lineage. We found that levels of *mtp* transcript were upregulated 14-fold in stationary phase Erdman cultures and 22-fold in stationary HN878 cultures relative to logarithmic phase Erdman cultures (Fig. 1). This growth phase-dependent expression of *mtp* in both strains suggests that the function of MTP is more important for Mtb in stationary phase compared to logarithmic phase. The levels of *mtp* in logarithmic phase were similarly low in Erdman and HN878 (with average Ct values of 25.3 and 26.4 in qRT-PCR analyses, respectively), but the induction of *mtp* in response to stationary phase was significantly more robust in HN878, suggesting that MTP may play a greater role in stationary phase in the HN878 strain (Fig. 1). In other bacterial pathogens, pili and curli are known to contribute to biofilm formation (DePas

et al., 2013; Flores-Mireles *et al.*, 2015; Mandlik *et al.*, 2008; Nallapareddy *et al.*, 2006; Telford *et al.*, 2006). Stationary phase mycobacteria share characteristics with bacteria grown in biofilms, including that cells growing under both conditions replicate more slowly, are phenotypically heterogeneous, are more nutrient starved and are more tolerant to a variety of stresses than their logarithmic counterparts (Richards & Ojha, 2014; Smeulders *et al.*, 1999). This suggests that some of the pathways active in stationary bacteria will also be active in bacteria within a biofilm. With the similarities between stationary phase and biofilm mycobacteria and the known contribution of pili to biofilms in other bacterial species in mind, we next investigated the expression of *mtp* in Mtb Erdman during *in vitro* biofilm formation. WT Mtb Erdman was inoculated into Sauton's medium and culture vessels were closed tightly to restrict oxygen for 3 weeks prior to venting, after which the pellicle biofilm robustly developed at the air–liquid interface (performed similarly as in Ojha *et al.*, 2008). We found that *mtp* transcripts were upregulated in 2-week but not in 3-week biofilm cultures relative to logarithmic phase planktonic cultures (Fig. 1).

mtp expression has strain-specific effects on biofilm formation

mtp expression in biofilms and the established contribution of pili and curli to biofilm formation in other bacteria led us to explore whether MTP plays a role in biofilm formation in Mtb Erdman and HN878 strains. To investigate a potential role for MTP in Mtb biofilm formation, we first engineered the genetic mutants Δ*mtp*, Δ*mtp*+*mtp* complemented strain and Δ*mtp*+empty vector control strain in the Mtb Erdman background (Fig. S1). The Δ*mtp* mutant was confirmed by Southern blot analysis (Fig. 2a). WT or *mtp* mutant strains of Mtb were inoculated into Sauton's medium and culture vessels were closed tightly to restrict oxygen for 3 weeks prior to venting, after which pellicle biofilm development was monitored weekly. Our results in Mtb Erdman show that the Δ*mtp* strain is not defective in biofilm formation relative to the WT or the vector control (Fig. 2b, c). Despite the result that disruption of *mtp* in Erdman resulted in normal pellicle formation, the complemented Δ*mtp*+*mtp* strain formed a more robust pellicle than any of the other strains, as seen by visualizing biofilm formation (Fig. 2b) and measuring crystal violet staining (Fig. 2c). We attribute this enhancement in pellicle biofilm formation by the Δ*mtp*+*mtp* strain to the constitutive expression of *mtp* under the non-endogenous promoter from the construct at the *attB* site. This effect on biofilm formation was specific for MTP, as the overexpression of an unrelated protein from the same promoter on the same construct integrated at the *attB* site did not result in enhanced pellicle formation (Weiss & Stallings, 2013). The biofilm cultures for each strain contained similar numbers of bacteria, indicating that the difference in pellicle formation was not due to higher numbers of bacteria in the Δ*mtp* +*mtp* strain biofilm than the others (Fig. S2a).

We also created an *mtp* deletion in HN878 (Fig. 2a). Unlike in Erdman, the HN878 Δ*mtp* (HNΔ*mtp*) strain is defective in pellicle biofilm formation relative to the HN878 WT strain (Fig. 2b, c). The pellicle of the HNΔ*mtp* strain eventually reached WT levels (Fig. S2b), indicating that the strain is capable of forming a pellicle but that pellicle formation is delayed. Variations in pellicle formation among Erdman and HN878 strains in this study were not due to differences in growth, as all strains grew similarly in planktonic growth curves (Fig. S2c, d). During our investigations into a role for MTP in biofilm formation, a separate group reported that MTP contributes to biofilm formation in the Mtb V9124 strain, which is a drug-susceptible clinical isolate of the KZN family (Ramsugit *et al.*, 2013). Together, our data in HN878 and Erdman combined with Ramsugit *et al.*'s study in V9124 show that MTP can contribute to biofilms in Mtb, but the extent to which MTP is necessary for pellicle biofilm formation depends on the strain.

MTP is reported to share physical characteristics with curli, including fibre appearance upon microscopic analysis and insolubility in sodium dodecyl sulfate (Alteri *et al.*, 2007; Blanco *et al.*, 2012). Defects in curli formation in other bacteria are associated with defective diazo dye CR binding and smooth rather than rugose colony biofilm morphology (Barnhart & Chapman, 2006; DePas *et al.*, 2013). Colony morphology in Mtb is also linked to virulence, as strains that lack the typical structured morphology observed in WT Mtb colonies have reduced survival in macrophages and are avirulent in guinea pigs (Giovannini *et al.*, 2012; Middlebrook *et al.*, 1947). We spotted 5 μl of stationary phase Mtb onto 7H10 agar plates supplemented with CR and analysed the formation of rugose colony biofilms after 3 weeks of growth. We did not observe any difference in rugose colony biofilm morphology in any of the *mtp* mutants relative to the WT control (Fig. 2d). Neither Erdman Δ*mtp* nor HNΔ*mtp* had defects in CR binding, and HNΔ*mtp* actually appeared more red than HN878 WT. Notably, these studies also indicated that Mtb does not bind CR to the same degree as other organisms, such as *Escherichia coli* (Barnhart & Chapman, 2006).

mtp expression does not correlate with the abundance of cell-associated extracellular structures visualized by TEM

The absence of effects on CR binding raised the question of the presence and the nature of MTP curli-like pili, which have not been confirmed across the field of Mtb research and have only been studied microscopically in two publications (Alteri *et al.*, 2007; Ramsugit *et al.*, 2013). The structures referred to as the curli-like MTP in each of these publications appear morphologically diverse within a single paper and across the two publications. Alteri *et al.* (2007) reported that 10 % of mycobacterial cells (from H37Rv, H37Ra and CDC1551 strains) produced MTP structures, while Ramsugit *et al.* (2013) reported that 80 % of WT V9124 were 'piliated'. Therefore, in order to determine

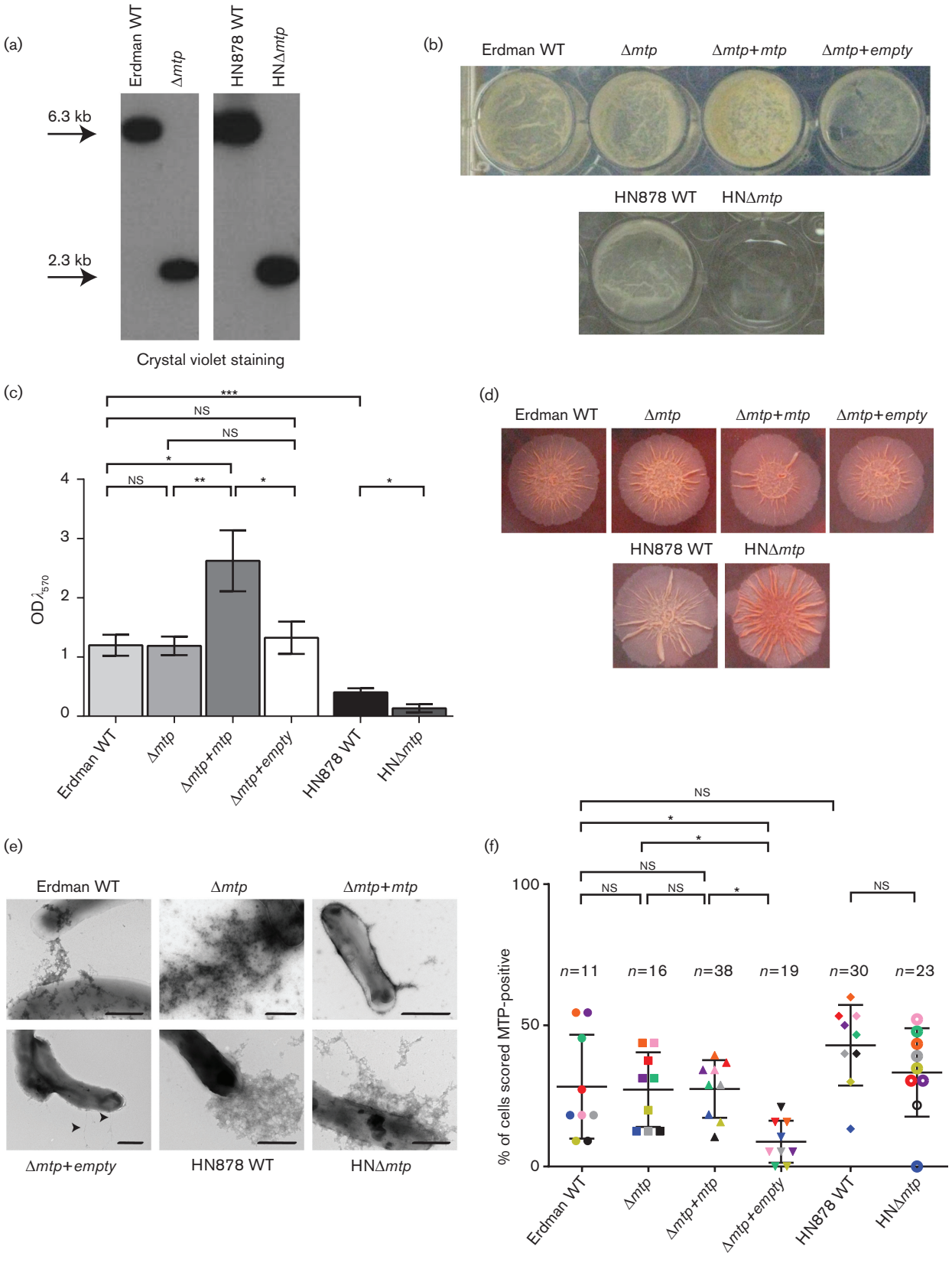

Fig. 2. Biofilm formation of *mtp* deletion strains. (a) Southern blot analysis of WT and *mtp* deletion mutants in Erdman and HN878 strains. Genomic DNA was digested with EcoRV, which yields a 6.3 kb WT band or a 2.3 kb Δ*mtp* band. (b) Pellicle

biofilm formation of Erdman WT, Δ*mtp*, Δ*mtp*+*mtp*, Δ*mtp*+*empty*, HN878 WT and HNΔ*mtp* strains in 24-well plates. (c) Crystal violet quantification of pellicle biofilm formation from 96-well plates. Each bar represents triplicate data across three independent experiments. (d) Rugose colony biofilm morphology of Erdman WT, Δ*mtp*, Δ*mtp*+*mtp*,Δ*mtp*+*empty*, HN878 WT and HNΔ*mtp* on CR 7H10 plates. (e) Representative negative staining TEM images from each strain to illustrate the cell-associated structures observed. Scale bars represent 500 nm. (f) Percentage of cells scored as 'MTP-positive' across the six bacterial strains by nine blinded reviewers. Each coloured symbol represents a reviewer. The *n* numbers displayed above each sample dataset correspond to the total number of individual cells for each strain that were scored. Statistical significance was analysed by ANOVA and Tukey's multiple comparison test. **P*<0.05, ***P*<0.01 and ****P*<0.001; NS, not significant.

whether our panel of mutants differed in the presence of curli-like, cell-associated extracellular structures, we performed uranyl acetate negative staining followed by TEM of samples from pellicles and rugose colony biofilms (Fig. 2e, f). Due to controversy in the field over the existence of curli-like MTP and the scarce characterization of MTP itself, we employed nine individual blinded reviewers to score 130 electron microscopic images across the six WT and mutant strains for what we termed 'MTP-positive' cells. Reviewers were trained to look for 'MTP-positive' cells based on the aggregative, string-like, cell-associated extracellular structures found in figures in the two previous publications (Alteri *et al.*, 2007; Ramsugit *et al.,* 2013). Examples of what would have scored as 'MTP-positive' cells from each strain are presented in Fig. 2e. Fig. 2f displays the percentage of cells scored as 'MTP-positive' in each strain by each of the nine reviewers, with each reviewer represented by a certain colour symbol. Fig. 2f demonstrates that even with variability in what is considered 'MTP-positive' across reviewers, the three strains that are genetically deficient for *mtp* (Δ*mtp*, Δ*mtp*+*empty*, HNΔ*mtp*) are still viewed as having 'MTP-positive' cells based on the presence of cell-associated extracellular structures similar to those reported in previously published work. The only statistically significant comparisons are with Δ*mtp*+*empty*, which on average has relatively lower reports of 'MTP-positive' cells but still had examples of cell-associated extracellular structures. These data show that phenotypes associated with these strains correlate with the presence, absence or constitutive expression of *mtp* but do not correlate with differences in the abundance of cell-associated extracellular structures.

Constitutive expression of *mtp* enhances tolerance to INH

Biofilm cultures of Mtb harbour increased numbers of antibiotic-tolerant bacteria relative to planktonically grown Mtb (Ojha *et al.*, 2008). To investigate whether the different pellicle biofilm phenotypes in the Erdman WT, Δ*mtp*, Δ*mtp* +*mtp* and Δ*mtp*+*empty* strains (Fig. 2) would affect antibiotic tolerance, we performed a biofilm stress assay with INH. Biofilm cultures were started and carried out as usual for 3 weeks. Upon aeration at the 3-week time point, 50 μg ml^{-1} INH, 100 μg ml^{-1} INH or water control was added to the culture by pipetting underneath the premature pellicle (Fig. 3a). Bacteria were harvested from each well after 2 weeks of INH treatment (after a total of 5 weeks under the biofilm culturing conditions) and plated for c.f.u. Relative to the untreated control for each strain, significantly more bacteria survived 50 μg ml^{-1} and 100 μg ml^{-1} INH treatment in the Δ*mtp*+*mtp* strain than any of the other strains (Fig. 3b). This difference in survival between strains after INH treatment was not observed in planktonic stress assays (Fig. S2e), indicating that the increased tolerance to INH in the Δ*mtp*+*mtp* strain is specific to Mtb grown under the biofilm condition. This could be due to either the enhanced biomass of the Δ*mtp*+*mtp* pellicle itself or MTP providing some other benefit under the nutrient-poor, slow-growing condition of the biofilm. These data together demonstrate that while loss of MTP does not sensitize Mtb to INH, the constitutive expression of MTP can enhance drug tolerance of Mtb grown under biofilm conditions.

MTP is not required for Mtb survival but can impact histopathology in a mouse model of infection

Mtb growing in biofilms share many characteristics with Mtb growing in the host during chronic infection, including decreased replication rates, decreased nutrient availability and increased stress tolerance as seen by an increase in persister cell formation relative to planktonic culture (Ojha *et al.*, 2008; Richards & Ojha, 2014). Multiple groups have also reported the observation of extracellular communities of Mtb that resemble biofilms during infection (Lenaerts *et al.*, 2007; Orme, 2014; Wong & Jacobs, 2016), although this is highly debated. These necrosis-associated extracellular clusters (NECs) of Mtb were initially observed in guinea pigs in an extracellular microenvironment that is present at the acellular rim of residual primary lesion necrosis (Lenaerts *et al.*, 2007). Lung lesions in the guinea pig model display necrosis, mineralization and hypoxia, and thus are more similar to human lesions than those found in the C57Bl/6 mouse model (Lenaerts *et al.*, 2007). As an alternative to C57Bl/6 mice, populations of necrosis-associated extracellular bacteria in micro-environments similar to the guinea pig model have been found in C3HeB/FeJ mice, which form lesions that are both hypoxic and necrotic (Driver *et al.,* 2012; Harper *et al.*, 2012). In humans, necrosis leads to pulmonary cavitation, which is a hallmark of the most common form of TB (Wong & Jacobs, 2016).

The growing interest in understanding the contribution of biofilm-like NECs to Mtb virulence *in vivo*, our findings that MTP contributes to biofilm formation and drug

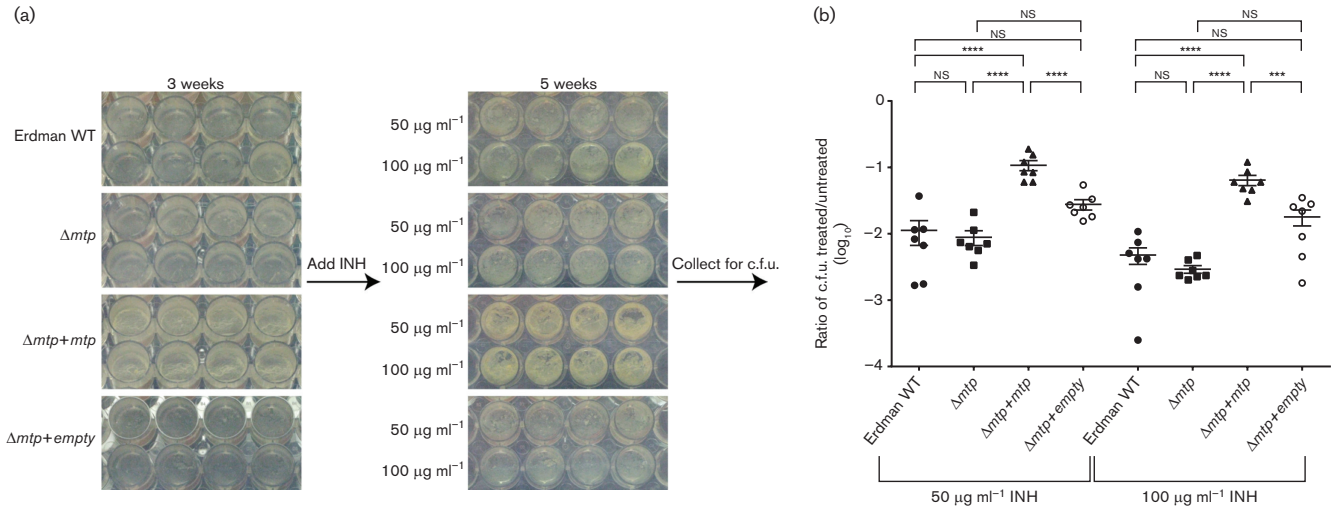

Fig. 3. INH tolerance during biofilm growth. (a) Left: pellicle biofilm formation of Erdman WT, Δ*mtp*, Δ*mtp*+*mtp* and Δ*mtp* +*empty* at 3 weeks, prior to the addition of INH. Right: pellicle biofilm formation in the same wells 2 weeks after starting INH treatment. Wells in the top row of the image for each strain were treated with 50 μg ml^{-1} INH, and wells in the bottom row were treated with 100 μg ml^{-1} INH. (b) Survival of Erdman WT, Δ*mtp*, Δ*mtp*+*mtp* and Δ*mtp*+*empty* after 50 μg ml^{-1} or 100 μg ml^{-1} INH treatment under biofilm conditions. Data are expressed as a ratio relative to the average of untreated samples for each strain. Each symbol represents a single replicate and shown are a total of six to seven biological replicates across two independent experiments. Statistical significance was analysed by ANOVA and Tukey's multiple comparison test. ***P<0.001, ****P<0.0001; NS, not significant.

tolerance (Figs. 2 and 3) and the multiple studies demonstrating attachment defects of *mtp* mutants *in vitro* (Alteri *et al.*, 2007; Ramsugit & Pillay, 2014; Ramsugit *et al.*, 2016) together begged the question of whether MTP contributes to Mtb virulence in animal models. To investigate the role of MTP in Mtb pathogenesis, we infected C3HeB/FeJ mice, which form necrotic lesions, with Erdman WT, Δ*mtp* and Δ*mtp*+*mtp* Mtb strains by the aerosol route. After infection, mouse lungs and spleens were harvested and c.f.u. were enumerated at various time points during both the acute and persistent phases of infection (Fig. 4a, b). The Δ*mtp* strain was not attenuated at any time point in the lung or spleen. In fact, at 56 days post-infection (d.p.i.), the Δ*mtp* strain had significantly higher c.f.u. in both organs compared to the other two strains. These data indicate that losing *mtp* expression does not hinder bacterial survival in the C3HeB/FeJ mouse model of infection. Furthermore, the Δ*mtp*+*mtp* strain showed no statistical difference in bacterial burden relative to WT Mtb. Therefore, despite the increased pellicle formation and subsequent INH tolerance of the Δ*mtp*+*mtp* strain *in vitro*, this does not confer a fitness advantage in the mouse. We also found similar c.f.u. trends when we infected C57Bl/6 mice (Fig. S3), supporting that MTP is not required for Mtb colonization, spread or survival in mice.

In addition to monitoring bacterial burden, lungs were also collected for histological analysis. Lungs from C3HeB/FeJ mice at 56 d.p.i. with Erdman WT, Δ*mtp* or Δ*mtp*+*mtp* were processed and two consecutive sections were stained for H&E or acid-fast bacilli (Fig. 4c–q). We found extracellular acid-fast -positive bacteria present in lungs of all the mice examined. Two types of lesion were found in the lungs of C3HeB/FeJ mice. The first and more common type of lesion is very inflamed but is less structured, and it contains both intracellular and extracellular bacteria (Fig. 4e, h and k). This type of unencapsulated lesion was present in every lung section from each of the different Mtb strain infections (Fig. 4c–k). The second type of lesion we observed contained distinct margins and has previously been referred to as an encapsulated lesion (Driver *et al.*, 2012) (Fig. 4l–q). The encapsulated lesions were only present in the lungs infected with Erdman WT or Δ*mtp* strains. In addition to intracellular bacteria, encapsulated lesions were full of extracellular bacteria, which were often present in clusters (Fig. 4n, q). The prevalence of encapsulated lesions corresponded to the level of bacterial burden at that time point. The strain with the fewest c.f.u. at this 56 d.p.i. time point, Δ*mtp*+*mtp*, had no lungs that contained encapsulated lesions (n=12, 0 %). The Erdman WT strain, which had intermediate c.f.u. levels at the 56 d.p.i. time point, had one lung section that contained one encapsulated lesion (n=12, 8.3 %). Δ*mtp* infection led to the highest bacterial burden at 56 d.p.i. and resulted in sections from two separate lungs that each contained two encapsulated lesions (n=6, 33 %). These studies confirm the presence of clustered extracellular bacteria in the C3HeB/FeJ mouse model of TB for all Erdman strains tested, and suggest that the expression levels of *mtp* may influence histopathological features. However,

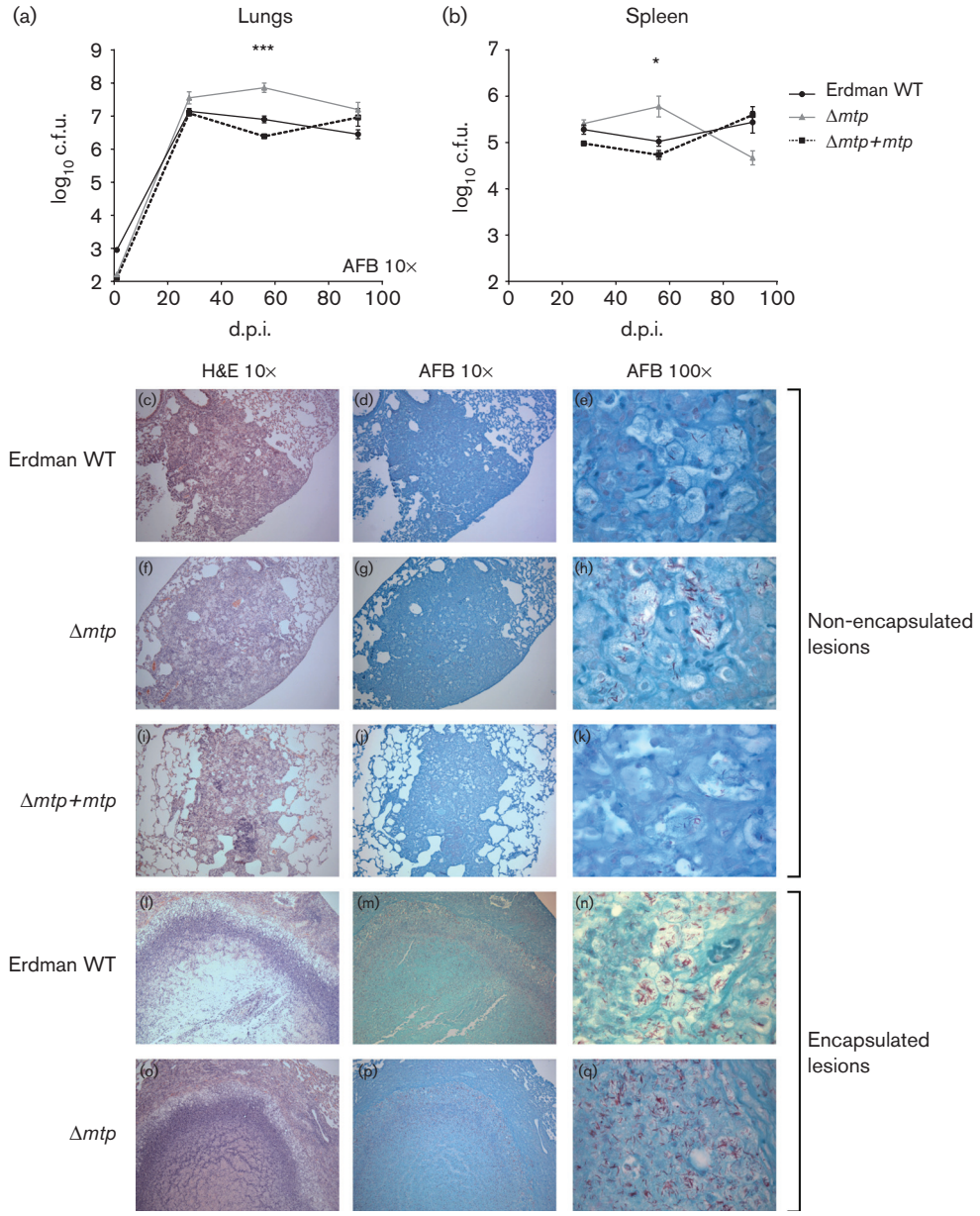

Fig. 4. Pathogenesis of *mtp* mutants in C3HeB/FeJ mice. Bacterial titres in the (a) lungs and (b) spleens of C3HeB/FeJ mice infected with Erdman WT (black filled circles), Δ*mtp* (grey filled triangles) or Δ*mtp*+*mtp* (black filled squares connected by a broken line) strains by the aerosol route. The Erdman WT and Δ*mtp*+*mtp* infections were performed twice with two or three mice per time point per infection. The data represent the average of two experiments. The Δ*mtp* infection was performed once with three mice per time point. Statistical significance across groups determined by ANOVA, **P*<0.05 and ****P*<0.001. (c–q) Histology of lungs from 56 d.p.i. with Erdman WT (c–e and l–n), Δ*mtp* (f–h and o–q) and Δ*mtp*+*mtp* (i–k). Consecutive sections were stained with either H&E (c, f, i, l and o) or a stain for acid-fast bacilli (AFB) (d–e, g–h, j–k, m–n and p–q) and visualized at either the ×10 objective (c, d, f, g, i, j, l, m, o and p) or the ×100 objective (e, h, k, n and q) on a light microscope. The top three rows represent the more prevalent, less-structured, unencapsulated lesions found during all infections. The fourth row depicts an encapsulated lesion from Erdman WT infection, while the last row depicts an encapsulated lesion from Δ*mtp* infection.

since the presence of encapsulated lesions correlated not only with *mtp* expression but also with bacterial burden, the source of the phenotype is uncertain. Therefore, it is possible that *mtp* expression levels impact immune responses to the infection; however, the finding that MTP is not required for Mtb Erdman infection, spread and survival

is contrary to what was predicted from *in vitro* adherence studies (Ramsugit *et al.*, 2016).

The predicted Flp pilus is not required for biofilm formation or Mtb survival in C57Bl/6 mice

With an interest in characterizing the role of potential pili in Mtb, we generated two Mtb Erdman genetic deletions targeting components of the *tad* operon, which encodes the predicted type IV Flp pilus (Δ*tadAB* and Δ*tadC-flp*; Fig. 5a). Mutant strains were confirmed via Southern blot analysis (Fig. 5b). We used these mutants to interrogate the contribution of the *tad* operon to Mtb physiology and virulence. Since *tad*-encoded Flp pili in other bacteria are required for adherence and autoaggregation (Planet *et al.*, 2003), we sought to assess the ability of Mtb *tad* mutants to form biofilms. Cultures of WT or *tad* mutant strains of Mtb were used to inoculate biofilm cultures as described before. No differences were observed in pellicle biofilm development of the *tad* mutants compared to the WT control (Fig. 5c), demonstrating that the proteins encoded by the *tad* operon do not play a role in biofilm formation under these conditions.

Given that type IV pili in other bacteria have been associated with host cell adhesion and virulence (Craig *et al.*, 2004; Schreiner *et al.*, 2003), we wanted to investigate the potential contribution of the *tad* locus to Mtb virulence. To do this, we infected C57Bl/6 mice with Erdman WT, Δ*tadAB* or Δ*tadC-flp* strains of Mtb and measured pulmonary and splenic Mtb burden at various time points post-infection. Neither of the Mtb *tad* mutant strains was attenuated in this model (Fig. 5d, e). The number of Mtb c.f.u. in the lungs and spleens of infected mice showed no statistically significant differences between the strains tested across all time points, except at 35 d.p.i. when Δ*tadC-flp* had a small but significant increase in bacterial burden in the lung (Fig. 5d). The unattenuated colonization and spread of the *tad* mutants in mice and normal biofilm formation *in vitro* demonstrate that the predicted Flp pilus is not required for the ability of Mtb to form community associations in culture or to infect in this mouse model.

DISCUSSION

For the most part, how Mtb-encoded adhesins contribute to virulence has remained a mystery. One of the only adhesins that has been demonstrated to have a role in Mtb pathogenesis is the heparin-binding haemagglutinin adhesion protein (HBHA), which recognizes receptors on epithelial cells (Pethe *et al.*, 2000). HBHA was shown to be dispensable for colonization of mouse lungs and binding to phagocytic cells like macrophages, but was important for epithelial cell interactions and extrapulmonary spread of Mtb in a mouse model of infection (Pethe *et al.*, 2001). It has recently been suggested that one or more predicted mycobacterial pili may play a role in Mtb adhesion to host tissue and virulence. In the case of MTP, this suggestion has been primarily supported by *in vitro* biofilm, attachment and invasion assays (Alteri *et al.*, 2007; Ramsugit *et al.*, 2013, 2016; Ramsugit & Pillay, 2014). Despite the uncertain contribution of MTP to virulence, these studies have spurred other groups to study MTP and MTP has been included as important for Mtb adherence in reviews on the subject (Govender *et al.*, 2014; Hosseini *et al.*, 2014; Ramsugit & Pillay, 2015). In addition to MTP, a putative pilus encoded by the widely conserved *tad* locus has also been suggested to be expressed and important in virulence (Alteri, 2005; Govender *et al.*, 2014). However, to the best of our knowledge, the actual contribution of these factors to Mtb virulence had not been assessed before our study.

In this work, we found that MTP can contribute to *in vitro* pellicle biofilm formation in a strain-specific manner (Fig. 2). Mtb HN878 (Fig. 2) and V9124 (Ramsugit *et al.*, 2013) strains require MTP for normal biofilm formation. The Mtb Erdman strain does not require MTP to form biofilms, but pellicle biofilm formation is more robust in an Erdman strain constitutively expressing MTP (Fig. 2). This enhanced pellicle in the Δ*mtp+mtp* strain leads to increased tolerance to INH (Fig. 3). Despite previous studies suggesting that MTP may be a better adhesin than HBHA (Ramsugit *et al.*, 2016), we found that the enhanced pellicle in the Δ*mtp+mtp* strain does not translate to enhanced infection and spread in mice, nor does the deletion of *mtp* attenuate the bacteria during infection (Figs 4 and S3). In addition, we show that the *tad* locus genes are not required for Mtb Erdman virulence in C57Bl/6 mice, and at certain time points during infection the Δ*mtp* and Δ*tadC/flp* strains actually had higher bacterial titres in infected lungs (Figs 4, 5 and S3).

While further work is required to understand why these deletion strains are at times more virulent, one could propose that the host immune system may target these molecules, so a decrease in antigen may actually be advantageous. In support of this, infection of C3HeB/FeJ mice with Erdman WT, Δ*mtp* or Δ*mtp+mtp* resulted in varying levels of histopathology at 56 d.p.i. (Fig. 4c–q), where Δ*mtp+mtp* elicited the fewest number of encapsulated lesions and Δ*mtp* elicited the most. However, it is not clear whether the difference in histopathology is due to differences in bacterial burden at 56 d.p.i. or due to differences in MTP expression. For instance, loss of *mtp* expression could lead to the formation of a higher number of encapsulated lesions where the bacteria replicate at high numbers extracellularly, contributing to the higher bacterial burden. Alternatively, loss of *mtp* expression could lead to a growth advantage and higher bacterial burden, which then leads to the formation of more encapsulated lesions. Whichever may be the case, different levels of *mtp* expression affect lesion architecture at 56 d.p.i., but MTP is not required for Mtb to survive in mice.

There are also multiple steps in human Mtb infection that are not mirrored in mice, including dystrophic mineralization (Driver *et al.*, 2012), pulmonary cavitation (Wong &

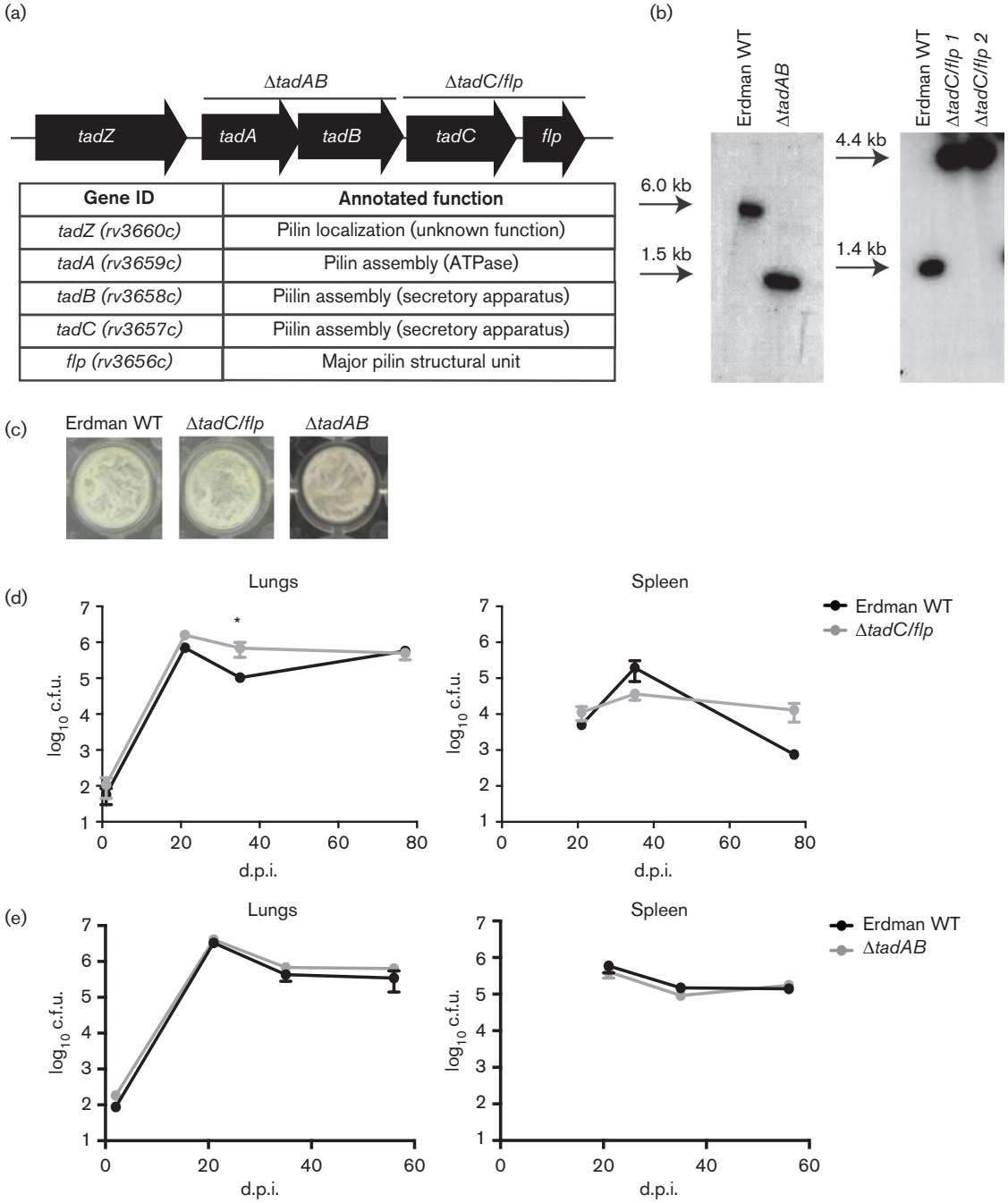

Gene ID	Annotated function
tadZ (rv3660c)	Pilin localization (unknown function)
tadA (rv3659c)	Pilin assembly (ATPase)
tadB (rv3658c)	Piilin assembly (secretory apparatus)
tadC (rv3657c)	Piilin assembly (secretory apparatus)
flp (rv3656c)	Major pilin structural unit

Fig. 5. Effects of disruption of the *tad* locus on Mtb physiology and virulence. (a) Genetic organization of the *tad* operon maintained in the Mtb genome. Annotated functions of the *tad* genes are listed in the table. Regions selected for deletion are marked with black bars and labelled with the name of the deletion strain above the bar. (b) Southern blot analysis of *tad* deletion mutants. Left: for Δ*tadAB*, mutant and WT strain genomic DNA were digested with SacI, resulting in a WT 6.0 kb band or a 1.5 kb Δ*tadAB* band. Right: digestion with NheI yields a 1.4 kb WT band or a 4.4 kb Δ*tadC/flp* band. (c) Pellicle biofilm formation of *tad* mutants in 96-well plates. (d) Bacterial titres in the lungs (left) or spleen (right) of C57Bl/6 mice infected by the aerosol route with Erdman WT (black filled circles) or Δ*tadC/flp* (grey filled circles). Erdman WT and Δ*tadC/flp* infections were performed twice with three mice per time point per experiment; one experiment is shown. (e) Bacterial titres in the lungs (left) or spleen (right) of C57Bl/6 mice infected by the aerosol route with Erdman WT (black filled circles) or Δ*tadAB* (grey filled circles). The Δ*tadAB* infection was performed once with three mice per time point. Statistical significance between two groups was determined by Student's *t*-test; **P*<0.05.

Jacobs, 2016) and transmission to new hosts. It is possible that MTP and the Flp pilus locus may contribute to these stages of pathogenesis. An additional factor to consider in the discussion of the role of MTP in virulence is Mtb strain differences. In future studies, it will be interesting to explore whether MTP is required for infection and spread in the HN878 and V9124 strains, where loss of *mtp* leads to defects in pellicle biofilm formation (Fig. 2 and Ramsugit *et al.*, 2013). *mtp* transcript levels are also more upregulated in stationary phase relative to log phase cultures in HN878 than in Erdman, perhaps suggesting that MTP plays a more important role in HN878 physiology (Fig. 1). In addition, while the functions of MTP remain elusive, the combined pieces of data that sera from TB patients contain antibody against MTP (Alteri *et al.*, 2007), and that the *mtp* gene is highly conserved in Mtb complex bacteria but not in non-tuberculous mycobacteria, collectively support that MTP could be a potentially useful biomarker for Mtb, as has previously been suggested (Govender *et al.*, 2014; Naidoo *et al.*, 2014).

In general, analysis of *mtp* mutants is complicated by the lack of correlation with the abundance of cell-associated extracellular structures in our strains. Before this report, the presence and nature of pili in Mtb had only been reported by two research groups and are currently debated. Our data generated by nine blinded reviewers scoring over 130 electron microscopy images suggest that the structures shown in previous publications may not represent MTP (Alteri *et al.*, 2007; Ramsugit *et al.*, 2013), but instead may represent an unidentified feature such as adherent extracellular matrix components. However, different Mtb strains have been used in the various studies which could contribute to the variability in findings. Thus, further studies are required to truly understand the existence of pili in Mtb. Regardless, the previous studies and our own work presented herein support roles for the protein encoded by the *mtp* gene in biofilm formation and subsequent INH tolerance, as well as a potential role in promoting a certain lesion architecture during mouse infection.

The question of how Mtb adheres to different host tissues *in vivo* still stands. Mtb encodes many other adhesins and suggested adhesins (as reviewed in Govender *et al.*, 2014), but the effects of most of these proteins are yet to be determined *in vivo*. This large number of predicted adhesins also raises the question of redundancy, which could confound analyses of single mutations. In addition, with about half of the Mtb genome encoding hypothetical proteins that have not been studied (Mazandu & Mulder, 2012), it cannot be ruled out that Mtb encodes novel factors important for host cell adherence that have yet to be identified. In conclusion, although neither MTP nor Flp are required for infection and spread in mice, the questions of how Mtb adheres and how that adherence relates to pathogenesis are important and remain wide open for future study.

ACKNOWLEDGEMENTS

We thank Dr Ashley Garner and Jeremy Huynh of Washington University in St. Louis for careful reading of the manuscript and providing insightful feedback. We also thank Dr Wandy Beatty and Dr Bryan Anthony at the Molecular Microbiology Imaging Facility in the Department of Molecular Microbiology at Washington University School of Medicine for their assistance in imaging samples. The Pulmonary Morphology Core is supported by an Asthma and Allergic Disease Cooperative Research Center grant from the National Institute of Allergy and Infectious Diseases of the NIH under award number U19AI070489. C. L. S. is supported by a Beckman Young Investigator Award from the Arnold and Mabel Beckman Foundation and an Interdisciplinary Research Initiative grant from the Children's Discovery Institute of Washington University and St. Louis Children's Hospital. K. M. M. is supported by the NIH Infectious Disease Training grant no. AI007172 and the Stephen I. Morse Graduate Fellowship. A. C. P. is supported by the W. M. Keck Foundation Fellowship in Molecular Medicine. K. F. is supported by a pilot award from the Center for Women's Infectious Disease Research at Washington University School of Medicine. J. M. K. is supported by a National Science Foundation Graduate Research Fellowship DGE-1143954 and the National Institute of General Medical Sciences Cell and Molecular Biology Training grant no. GM007067.

REFERENCES

Alteri, C. J. (2005). Novel pili of Mycobacterium tuberculosis. *PhD thesis*. Tucson, AZ: University of Arizona.

Alteri, C. J., Xicohténcatl-Cortes, J., Hess, S., Caballero-Olín, G., Girón, J. A. & Friedman, R. L. (2007). *Mycobacterium tuberculosis* produces pili during human infection. *Proc Natl Acad Sci U S A* **104**, 5145–5150.

Barnhart, M. M. & Chapman, M. R. (2006). Curli biogenesis and function. *Annu Rev Microbiol* **60**, 131–147.

Barocchi, M. A., Ries, J., Zogaj, X., Hemsley, C., Albiger, B., Kanth, A., Dahlberg, S., Fernebro, J., Moschioni, M. & other authors (2006). A pneumococcal pilus influences virulence and host inflammatory responses. *Proc Natl Acad Sci U S A* **103**, 2857–2862.

Blanco, L. P., Evans, M. L., Smith, D. R., Badtke, M. P. & Chapman, M. R. (2012). Diversity, biogenesis and function of microbial amyloids. *Trends Microbiol* **20**, 66–73.

Connell, I., Agace, W., Klemm, P., Schembri, M., Mărild, S. & Svanborg, C. (1996). Type 1 fimbrial expression enhances *Escherichia coli* virulence for the urinary tract. *Proc Natl Acad Sci U S A* **93**, 9827–9832.

Craig, L., Pique, M. E. & Tainer, J. A. (2004). Type IV pilus structure and bacterial pathogenicity. *Nat Rev Microbiol* **2**, 363–378.

DePas, W. H., Hufnagel, D. A., Lee, J. S., Blanco, L. P., Bernstein, H. C., Fisher, S. T., James, G. A., Stewart, P. S. & Chapman, M. R. (2013). Iron induces bimodal population development by *Escherichia coli*. *Proc Natl Acad Sci U S A* **110**, 2629–2634.

Driver, E. R., Ryan, G. J., Hoff, D. R., Irwin, S. M., Basaraba, R. J., Kramnik, I. & Lenaerts, A. J. (2012). Evaluation of a mouse model of necrotic granuloma formation using C3HeB/FeJ mice for testing of drugs against *Mycobacterium tuberculosis*. *Antimicrob Agents Chemother* **56**, 3181–3195.

Flores-Mireles, A. L., Walker, J. N., Caparon, M. & Hultgren, S. J. (2015). Urinary tract infections: epidemiology, mechanisms of infection and treatment options. *Nat Rev Microbiol* **13**, 269–284.

Foster, T. J., Geoghegan, J. A., Ganesh, V. K. & Höök, M. (2014). Adhesion, invasion and evasion: the many functions of the surface proteins of *Staphylococcus aureus*. *Nat Rev Microbiol* **12**, 49–62.

Giovannini, D., Cappelli, G., Jiang, L., Castilletti, C., Colone, A., Serafino, A., Wannenes, F., Giacò, L., Quintiliani, G. & other authors (2012). A new *Mycobacterium tuberculosis* smooth colony reduces growth inside human macrophages and represses PDIM Operon gene expression. Does an heterogeneous population exist in intracellular mycobacteria? *Microb Pathog* **53**, 135–146.

Govender, V. S., Ramsugit, S. & Pillay, M. (2014). *Mycobacterium tuberculosis* adhesins: potential biomarkers as anti-tuberculosis therapeutic and diagnostic targets. *Microbiology* **160**, 1821–1831.

Harper, J., Skerry, C., Davis, S. L., Tasneen, R., Weird, M., Kramnik, I., Bishai, W. R., Pomper, M. G., Nuermberger, E. L. & Jain, S. K. (2012). Mouse model of necrotic tuberculosis granulomas develops hypoxic lesions. *J Infect Dis* **205**, 595–602.

Hosseini, H., Fooladi, A. A. I., Arjomandzadegan, M., Emami, N. & Bornasi, H. (2014). Genetics study and transmission electron microscopy of pili in susceptible and resistant clinical isolates of *Mycobacterium tuberculosis*. *Asian Pac J Trop Med* **7**, S199–S203.

Kachlany, S. C., Planet, P. J., Bhattacharjee, M. K., Kollia, E., DeSalle, R., Fine, D. H. & Figurski, D. H. (2000). Nonspecific adherence by *Actinobacillus actinomycetemcomitans* requires genes widespread in bacteria and archaea. *J Bacteriol* **182**, 6169–6176.

Kachlany, S. C., Planet, P. J., Desalle, R., Fine, D. H., Figurski, D. H. & Kaplan, J. B. (2001). *flp-1*, the first representative of a new pilin gene subfamily, is required for non-specific adherence of *Actinobacillus actinomycetemcomitans*. *Mol Microbiol* **40**, 542–545.

Khelef, N., Bachelet, C. M., Vargaftig, B. B. & Guiso, N. (1994). Characterization of murine lung inflammation after infection with parental *Bordetella pertussis* and mutants deficient in adhesins or toxins. *Infect Immun* **62**, 2893–2900.

Lee, J., Shin, S., Teng, C. H., Hong, S. J. & Kim, K. S. (2005). FimH adhesin of *Escherichia coli* K1 type 1 fimbriae activates BV-2 microglia. *Biochem Biophys Res Commun* **334**, 917–923.

Lenaerts, A. J., Hoff, D., Aly, S., Ehlers, S., Andries, K., Cantarero, L., Orme, I. M. & Basaraba, R. J. (2007). Location of persisting mycobacteria in a guinea pig model of tuberculosis revealed by r207910. *Antimicrob Agents Chemother* **51**, 3338–3345.

Mandlik, A., Swierczynski, A., Das, A. & Ton-That, H., Livny, J., Robins, W. P., Ritchie, J. M., Mekalanos, J. J. & Waldor, M. K. (2008). Pili in Gram-positive bacteria: assembly, involvement in colonization and biofilm development. *Trends Microbiol* **16**, 33–40.

Mazandu, G. K. & Mulder, N. J. (2012). Function prediction and analysis of *mycobacterium tuberculosis* hypothetical proteins. *Int J Mol Sci* **13**, 7283–7302.

Middlebrook, G., Dubos, R. J. & Pierce, C. (1947). Virulence and morphological characteristics of mammalian tubercle bacilli. *J Exp Med* **86**, 175–184.

Moorthy, S., Keklak, J. & Klein, E. A. (2016). Perspective: adhesion mediated signal transduction in bacterial pathogens. *Pathogens* **5**, E23.

Mulvey, M. A., Schilling, J. D. & Hultgren, S. J. (2001). Establishment of a persistent *Escherichia coli* reservoir during the acute phase of a bladder infection. *Infect Immun* **69**, 4572–4579.

Naidoo, N., Ramsugit, S. & Pillay, M. (2014). *Mycobacterium tuberculosis* pili (MTP), a putative biomarker for a tuberculosis diagnostic test. *Tuberculosis* **94**, 338–345.

Nallapareddy, S. R., Singh, K. V., Sillanpää, J., Garsin, D. A., Höök, M., Erlandsen, S. L. & Murray, B. E. (2006). Endocarditis and biofilm-associated pili of *Enterococcus faecalis*. *J Clin Invest* **116**, 2799–2807.

Nielsen, H. V., Guiton, P. S., Kline, K. A., Port, G. C., Pinkner, J. S., Neiers, F., Normark, S., Henriques-Normark, B., Caparon, M. G. & Hultgren, S. J. (2012). The Metal Ion-Dependent Adhesion Site Motif of the *Enterococcus faecalis* EbpA Pilin Mediates Pilus Function in Catheter-Associated Urinary Tract Infection. *mBio* **3**, e00177-12.

Nobbs, A. H., Lamont, R. J. & Jenkinson, H. F. (2009). Streptococcus adherence and colonization. *Microbiol Mol Biol Rev* **73**, 407–450.

O'Toole, G. A. & Kolter, R. (1998). Flagellar and twitching motility are necessary for *Pseudomonas aeruginosa* biofilm development. *Mol Microbiol* **30**, 295–304.

Ojha, A. K., Baughn, A. D., Sambandan, D., Hsu, T., Trivelli, X., Guerardel, Y., Alahari, A., Kremer, L., Jacobs, W. R. & Hatfull, G. F. (2008). Growth of *Mycobacterium tuberculosis* biofilms containing free mycolic acids and harbouring drug-tolerant mycobacteria. *Mol Microbiol* **69**, 164–174.

Orme, I. M. (2014). A new unifying theory of the pathogenesis of tuberculosis. *Tuberculosis* **94**, 8–14.

Parrish, N. M., Ko, C. G., Dick, J. D., Jones, P. B. & Ellingson, J. L. (2004). Growth, Congo Red agar colony morphotypes and antibiotic susceptibility testing of *Mycobacterium avium* subspecies paratuberculosis. *Clin Med Res* **2**, 107–114.

Pethe, K., Aumercier, M., Fort, E., Gatot, C., Locht, C. & Menozzi, F. D. (2000). Characterization of the heparin-binding site of the mycobacterial heparin-binding hemagglutinin adhesin. *J Biol Chem* **275**, 14273–14280.

Pethe, K., Alonso, S., Biet, F., Delogu, G., Brennan, M. J., Locht, C. & Menozzi, F. D. (2001). The heparin-binding haemagglutinin of *M. tuberculosis* is required for extrapulmonary dissemination. *Nature* **412**, 190–194.

Pizarro-Cerdá, J. & Cossart, P. (2006). Bacterial adhesion and entry into host cells. *Cell* **124**, 715–727.

Planet, P. J., Kachlany, S. C., Fine, D. H., DeSalle, R. & Figurski, D. H. (2003). The Widespread Colonization Island of *Actinobacillus actinomycetemcomitans*. *Nat Genet* **34**, 193–198.

Ramsugit, S., Guma, S., Pillay, B., Jain, P., Larsen, M. H., Danaviah, S. & Pillay, M. (2013). Pili contribute to biofilm formation in vitro in *Mycobacterium tuberculosis*. *Antonie Van Leeuwenhoek* **104**, 725–735.

Ramsugit, S. & Pillay, M. (2014). *Mycobacterium tuberculosis* Pili promote adhesion to and invasion of THP-1 macrophages. *Jpn J Infect Dis* **67**, 476–478.

Ramsugit, S. & Pillay, M. (2015). Pili of *Mycobacterium tuberculosis*: current knowledge and future prospects. *Arch Microbiol* **197**, 737–744.

Ramsugit, S., Pillay, B. & Pillay, M. (2016). Evaluation of the role of *Mycobacterium tuberculosis* pili (MTP) as an adhesin, invasin, and cytokine inducer of epithelial cells. *Braz J Infect Dis* **20**, 160–165.

Richards, J. & Ojha, A. (2014). Mycobacterial biofilms. In *Molecular Genetics of Mycobacteria*, Second Edition, Chapter 37 , pp. 773–784. Edited by G. Hatfull & W. Jacobs. Washington, DC: ASM Press.

Schreiner, H. C., Sinatra, K., Kaplan, J. B., Furgang, D., Kachlany, S. C., Planet, P. J., Perez, B. A., Figurski, D. H. & Fine, D. H. (2003). Tight-adherence genes of *Actinobacillus actinomycetemcomitans* are required for virulence in a rat model. *Proc Natl Acad Sci U S A* **100**, 7295–7300.

Smeulders, M. J., Keer, J., Speight, R. A. & Williams, H. D. (1999). Adaptation of *Mycobacterium smegmatis* to stationary phase. *J Bacteriol* **181**, 270–283.

Stallings, C. L., Stephanou, N. C., Chu, L., Hochschild, A., Nickels, B. E. & Glickman, M. S. (2009). CarD is an essential regulator of rRNA transcription required for *Mycobacterium tuberculosis* persistence. *Cell* **138**, 146–159.

Taylor, R. K., Miller, V. L., Furlong, D. B. & Mekalanos, J. J. (1987). Use of phoA gene fusions to identify a pilus colonization factor coordinately regulated with cholera toxin. *Proc Natl Acad Sci U S A* **84**, 2833–2837.

Telford, J. L., Barocchi, M. A., Margarit, I., Rappuoli, R. & Grandi, G. (2006). Pili in gram-positive pathogens. *Nat Rev Microbiol* **4**, 509–519.

Terao, Y. (2012). The virulence factors and pathogenic mechanisms of *Streptococcus pyogenes*. *J Oral Biosci* **54**, 96–100.

Tomich, M., Planet, P. J. & Figurski, D. H. (2007). The tad locus: postcards from the widespread colonization island. *Nat Rev Microbiol* **5**, 363–375.

Weiss, L. A. & Stallings, C. L. (2013). Essential roles for *Mycobacterium tuberculosis* Rel beyond the production of (p)ppGpp. *J Bacteriol* **195**, 5629–5638.

Wong, K.-W. & Jacobs, W. R. (2016). Postprimary Tuberculosis and Macrophage Necrosis: Is There a Big ConNECtion? *mBio* **7**, e01589-15.

WHO (2015). Global Tuberculosis Report. http://apps.who.int/iris/bitstream/10665/191102/1/9789241565059_eng.pdf.

Wright, K. J. & Hultgren, S. J. (2006). Sticky fibers and uropathogenesis: bacterial adhesins in the urinary tract. *Future Microbiol* **1**, 75–87.

Edited by: R. Manganelli

Figure 5—figure supplement 1. VWM-load-dependent strengthening of 1:2 CFS between high-α and β oscillations is observed in largely in sensorimotor, but also in attentional brain systems.Low-frequency (LF, left) and high-frequency (HF, right) CFS hubs and their connections for significant positive correlations with VWM memory load (Load condition) for CFS between high-α and β frequencies at ratio 1:2 (as in Figure 5, all illustration details as in Figure 4a).**DOI:** 10.7554/eLife.13451.020